

Asymptotic Effectiveness of a Catalyst Particle in the Form of a Hollow Cylinder

Rutherford Aris*

Dept. of Chemical Engineering and Material Science University of Minnesota, Minneapolis, MN 55455

Vemuri Balakotaiah

Dept. of Chemical Engineering University of Houston Houston, TX 77204

DOI 10.1002/aic.14222

Published online September 30, 2013 in Wiley Online Library (wileyonlinelibrary.com)

Significance

An explicit formula is presented for the effectiveness factor of a catalyst particle in the form of a hollow cylinder taking into account the reactant diffusion in the fluid phase of the cylindrical core and diffusion and reaction in the outer reactive annulus. The proper normalization to be used in the definition of the generalized Thiele modulus as well as the aspect ratios that lead to the highest effectiveness are also determined. © 2013 American Institute of Chemical Engineers *AICHE J.*, 59: 4020–4024, 2013

Keywords: diffusion, effectiveness factor, geometry factor, Aris numbers

Introduction

Westertep and his colleagues, Wijngaarden and Kronberg, have recently considered the hollow cylinder as a versatile form of catalyst particle for many catalytic reactions carried out in packed-beds.¹ From a practical point of view, a packed bed of hollow cylinders compares favorably with one packed with solid cylinders both in pressure drop and in accessibility of the catalyst. From a theoretical point of view, its geometry has important limiting cases of slab and solid cylinder, finite or infinite, some of which are simply connected and some not. The effectiveness of the hollow cylinder was first obtained by Gunn² and is mentioned in Aris,³ but the treatment by Wijngaarden et al.¹ is the most complete and their approximations are the most practical. In this note, we extend the work of Wijngaarden, Kronberg and Westertep (WKW) to the more realistic case by taking into account the reactant diffusion in the fluid phase of the cylindrical core and diffusion and reaction in the outer annulus.⁴ By making the diffusivity of the reactant very much larger in the core, we can approach the hollow cylinder limit (with Dirichlet boundary condition) considered by WKW and by shrinking the core we can approach the solid cylinder. We also analyze various geometrical limits, asymptotic forms and determine the optimum aspect ratios that lead to the most effective utilization of the catalyst.

Theory

We consider a porous catalyst particle in the form of a hollow cylinder of inner diameter $2a$, outer diameter $2b$ and length $2L$. Assuming a single step reaction $A \rightarrow B$ with linear kinetics in the annular region and only diffusion in the inner core, the steady-state reactant concentration profile satisfies the equations

$$D_e \nabla^2 C = k_0 C; \quad (r, \theta, x) \in \Omega_1 \quad (1)$$

$$D_m \nabla^2 C = 0; \quad (r, \theta, x) \in \Omega_2 \quad (2)$$

$$C = C_0; \quad \text{on } \partial\Omega. \quad (3)$$

Here, Ω_1 is the annular region in which reaction occurs, and Ω_2 is the interior cylindrical core while $\partial\Omega$ is the union of the exterior surface of the cylinder and the two circular disks of diameter $2b$. D_e is the effective diffusivity of the reactant in the porous catalyst, D_m is the diffusivity in the core, and k_0 is the first-order rate constant. Assuming azimuthal and axial symmetry and defining

$$\rho = \frac{r}{b}; \quad z = \frac{x}{L}; \quad \mu = \frac{a}{b}$$

$$\phi^2 = \frac{b^2 k_0}{D_e}; \quad \delta = \frac{D_e}{D_m}; \quad \lambda = \frac{L}{b} \quad (4)$$

$$U = 1 - \frac{C}{C_0} \quad (0 < \rho < \mu); \quad V = 1 - \frac{C}{C_0} \quad (\mu < \rho < 1)$$

Correspondence concerning this article should be addressed to V. Balakotaiah at bala@uh.edu.

*Rutherford Aris is deceased. Paper presented at the 1999 AIChE Annual Meeting.

the dimensionless form of the model is given by

$$\frac{1}{\rho} \frac{\partial}{\partial \rho} \left(\rho \frac{\partial U}{\partial \rho} \right) + \frac{1}{\lambda^2} \frac{\partial^2 U}{\partial z^2} = 0; 0 < z < 1, 0 < \rho < \mu \quad (5)$$

$$\frac{1}{\rho} \frac{\partial}{\partial \rho} \left(\rho \frac{\partial V}{\partial \rho} \right) + \frac{1}{\lambda^2} \frac{\partial^2 V}{\partial z^2} = \phi^2 V - \phi^2; 0 < z < 1, \mu < \rho < 1 \quad (6)$$

with boundary conditions

$$\frac{\partial U}{\partial z} = \frac{\partial V}{\partial z} = 0 \text{ at } z=0; U=V=0 \text{ at } z=1 \quad (7)$$

$$\frac{\partial U}{\partial \rho} = 0 \text{ at } \rho=0; V=0 \text{ at } \rho=1 \quad (8)$$

$$\frac{\partial U}{\partial \rho} = \delta \frac{\partial V}{\partial \rho} \text{ and } U=V \text{ at } \rho=\mu. \quad (9)$$

This last equation expresses the continuity of the flux and concentration at the boundary between the core and annulus. We can express the effectiveness factor by

$$\eta = 1 - \frac{1}{(1-\mu^2)} \int_0^1 \int_\mu^1 2V(\rho, z) \rho d\rho dz \quad (10)$$

The solution to the aforementioned model may be obtained using the Finite Fourier Transform. We note that the axial operator has normalized eigenfunctions

$$W_n(z) = \sqrt{2} \cos \left\{ \frac{(2n-1)\pi z}{2} \right\}; n=1, 2, \dots \quad (11)$$

Writing

$$U(\rho, z) = \sum_{n=1}^{\infty} U_n(\rho) W_n(z); V(\rho, z) = \sum_{n=1}^{\infty} V_n(\rho) W_n(z) \quad (12)$$

and taking inner product of Eqs. 5 and 6 with $W_n(z)$ gives

$$\frac{d^2 U_n}{d\rho^2} + \frac{1}{\rho} \frac{dU_n}{d\rho} - v_n^2 U_n = 0; \quad v_n^2 = \frac{(2n-1)^2 \pi^2}{4\lambda^2} \quad (13)$$

$$\frac{d^2 V_n}{d\rho^2} + \frac{1}{\rho} \frac{dV_n}{d\rho} - v_n^2 V_n = \phi^2 V_n - \phi^2 \langle 1, W_n(z) \rangle$$

$$\frac{dU_n}{d\rho} = 0 \text{ at } \rho=0, V_n=0 \text{ at } \rho=1$$

$$U_n = V_n, \frac{dU_n}{d\rho} = \delta \frac{dV_n}{d\rho} \text{ at } \rho=\mu \quad (14)$$

Here, $\langle \cdot, \cdot \rangle$ denotes the inner product

$$\langle 1, W_n(z) \rangle = \int_0^1 W_n(z) dz = \frac{2\sqrt{2}(-1)^{n-1}}{(2n-1)\pi}$$

Solving the aforementioned ordinary differential equations and applying the boundary conditions gives the radial functions

$$U_n(\rho) = c_1 I_0(v_n \rho) \quad (15)$$

$$V_n(\rho) = d_1 I_0(\psi_n \rho) + d_2 K_0(\psi_n \rho) + \frac{\phi^2}{\psi_n^2} \langle 1, W_n \rangle$$

where I_0 and K_0 are the modified Bessel functions,

$$\psi_n^2 = v_n^2 + \phi^2 = \frac{(2n-1)^2 \pi^2}{4\lambda^2} + \phi^2 \quad (16)$$

and the constants c_1 , d_1 , and d_2 can be evaluated from the boundary conditions. Substituting the solution $V(\rho, z)$ in the expression for the effectiveness factor, we obtain

$$\eta = 1 - \frac{8\phi^2}{\pi^2} \sum_{n=1}^{\infty} \frac{1}{(2n-1)^2 \psi_n^2} - \frac{16\phi^2}{\pi^2(1-\mu^2)} \sum_{n=1}^{\infty} \frac{E_n}{(2n-1)^2 \psi_n^3} \quad (17)$$

where

$$E_n = D_1 [I_1(\psi_n) - \mu I_1(\mu \psi_n)] + D_2 [\mu K_1(\mu \psi_n) - K_1(\psi_n)] \quad (18)$$

and the constants D_1 and D_2 are given by

$$D_1 I_0(\psi_n) + D_2 K_0(\psi_n) = -1$$

$$D_1 \alpha_1 + D_2 \alpha_2 = -v_n I_1(\mu \psi_n) \quad (19)$$

$$\alpha_1 = v_n I_1(\mu \psi_n) I_0(\mu \psi_n) - \delta \psi_n I_0(\mu v_n) I_1(\mu \psi_n)$$

$$\alpha_2 = v_n I_1(\mu \psi_n) K_0(\mu \psi_n) + \delta \psi_n I_0(\mu v_n) K_1(\mu \psi_n)$$

This form of the solution (without full simplification) is convenient for examining various limiting cases. For the general case, the algebra may be completed to obtain an explicit expression for the effectiveness factor

$$\eta = 1 - \frac{8\phi^2}{\pi^2(1-\mu^2)} \sum_{n=1}^{\infty} \frac{1-\mu^2+2\chi_n}{(2n-1)^2 \psi_n^2} \quad (20)$$

$$= \frac{\tanh \lambda \phi}{\lambda \phi} - \frac{16\phi^2}{\pi^2(1-\mu^2)} \sum_{n=1}^{\infty} \frac{\chi_n}{(2n-1)^2 \psi_n^2} \quad (21)$$

where

$$\chi_n =$$

$$\frac{2 - [\psi_n Q_0(\mu \psi_n, \psi_n) + \mu \psi_n Q_0(\psi_n, \mu \psi_n)] + \delta \frac{\psi_n^2 I_0(\mu v_n)}{v_n I_1(\mu v_n)} P_1(\mu \psi_n, \psi_n)}{\psi_n^2 [P_0(\psi_n, \mu \psi_n) + \delta \frac{\psi_n I_0(\mu v_n)}{v_n I_1(\mu v_n)} Q_0(\psi_n, \mu \psi_n)]} \quad (22)$$

and the various functions appearing above are defined by

$$P_0(a, b) = I_0(a) K_0(b) - I_0(b) K_0(a) \quad (23)$$

$$Q_0(a, b) = I_0(a) K_1(b) + I_1(b) K_0(a) \quad (24)$$

$$P_1(a, b) = I_1(a) K_1(b) - I_1(b) K_1(a) \quad (25)$$

We note that the computation of η as a function of ϕ , for any fixed values of μ , λ and δ involves only the evaluation of the Bessel functions. For the special case of $\delta = 0$, the terms containing δ in Eq. 22 can be dropped and the simplified expression reduces to that derived by WKW (after noting that $P_0(a, b) = -P_0(b, a)$).

Before analyzing the asymptotic behavior, we consider the normalization of the Thiele modulus or the effective diffusion length that leads to the expected asymptotic behavior. When $\delta > 0$, we define the effective diffusion length based on the reacting volume and the external area of the pellet on which the concentration is specified, i.e.

$$R_\Omega = \frac{V_p}{S_p} = \frac{2\pi \lambda b^3 (1-\mu^2)}{4\pi \lambda b^2 + 2\pi b^2 (1-\mu^2)} = b \frac{1}{\left[\frac{1}{\lambda} + \frac{2}{(1-\mu^2)} \right]}$$

Thus, the shape normalized Thiele modulus is defined by

$$\Phi^2 = \left(\frac{V_p}{S_p} \right)^2 \frac{k_0}{D_e} = \frac{\phi^2}{\left[\frac{1}{\lambda} + \frac{2}{(1-\mu^2)} \right]^2} \quad (26)$$

The aforementioned definition should be modified for the limiting case of $\delta = 0$ considered by WKW. In this case, since the reactant concentration is also specified at the interior surface, we define

$$R_\Omega = \frac{V_p}{S_p} = \frac{2\pi\lambda b^3(1-\mu^2)}{4\pi\lambda b^2 + 4\pi\lambda\mu b^2 + 2\pi b^2(1-\mu^2)} = b \frac{1}{\left[\frac{1}{\lambda} + \frac{2}{(1-\mu)} \right]} \quad (27)$$

and the shape normalized Thiele modulus by

$$\Phi_*^2 = \frac{\phi^2}{\left[\frac{1}{\lambda} + \frac{2}{(1-\mu)} \right]^2} \quad (28)$$

We note that

$$\frac{\Phi_*}{\Phi} = \begin{cases} \left[\frac{1 + \frac{2}{(1-\mu^2)}}{\frac{1}{\lambda} + \frac{2}{(1-\mu)}} \right] = \begin{cases} \frac{1}{1+\mu} & \text{for } \lambda \rightarrow \infty \text{ or } \mu \rightarrow 1 \\ 1 & \text{for } \lambda \rightarrow 0 \end{cases} \\ 1 & \text{for } \lambda \rightarrow 0 \end{cases} \quad (29)$$

Thus, except for the special case of $\mu = 0$ (solid cylinder) the two shape normalized Thiele moduli differ.

Asymptotic Behavior

For any fixed values of the geometrical parameters (or aspect ratios) μ and λ , and the diffusivity ratio δ , the asymptotic behavior of η for large ϕ may be obtained by noting that for $a, b \gg 1$

$$P_0(a, b) = P_1(a, b) = \frac{\sinh(a-b)}{\sqrt{ab}}; Q_0(a, b) = \frac{\cosh(a-b)}{\sqrt{ab}} \quad (30)$$

Using these relations, it may be shown that $\chi_n = -\frac{1}{\phi}$ (if $\phi \gg 1$, $\delta\phi \gg 1$) or $-\frac{(1+\mu)}{\phi}$ (if $\phi \gg 1$, $\delta\phi \ll 1$) and using this result in Eq. 21 leads to

$$\eta = \begin{cases} \left[\frac{1 + \frac{2}{(1-\mu)}}{\frac{1}{\lambda} + \frac{2}{(1-\mu)}} \right] \frac{1}{\phi} = \frac{1}{\Phi_*} & \text{for } \delta\phi \ll 1 \text{ and } \lambda\phi \gg 1 \\ \left[\frac{1 + \frac{2}{(1-\mu^2)}}{\frac{1}{\lambda} + \frac{2}{(1-\mu)}} \right] \frac{1}{\phi} = \frac{1}{\Phi} & \text{for } \delta\phi \gg 1 \text{ and } \lambda\phi \gg 1 \end{cases} \quad (31)$$

Thus, except for $\mu = 0$ (solid cylinder), the asymptotic behavior of the hollow cylinder for large Φ depends on the boundary condition used at the interior surface and the above definition of the shape normalized Thiele modulus leads to the expected asymptotic behavior ($\eta\Phi_* \rightarrow 1$ for $\delta\phi \ll 1$ and $\Phi_* \gg 1$ while $\eta\Phi \rightarrow 1$ for $\delta\phi \gg 1$ and $\Phi \gg 1$). We also note that for any $\delta > 0$, the condition $\delta\phi \ll 1$ is not satisfied for large ϕ , and, hence, the use of Dirichlet boundary condition at the interior surface is not justified from a physical point of view. (The same observation applies at the external boundary when the Biot number is fixed, but we do not consider this case here.)

Figure 1 shows a plot of η vs. Φ for a typical case $\delta = 0.1$, $\lambda = 1$ and three different values of μ (0.2, 0.5 and 0.9).

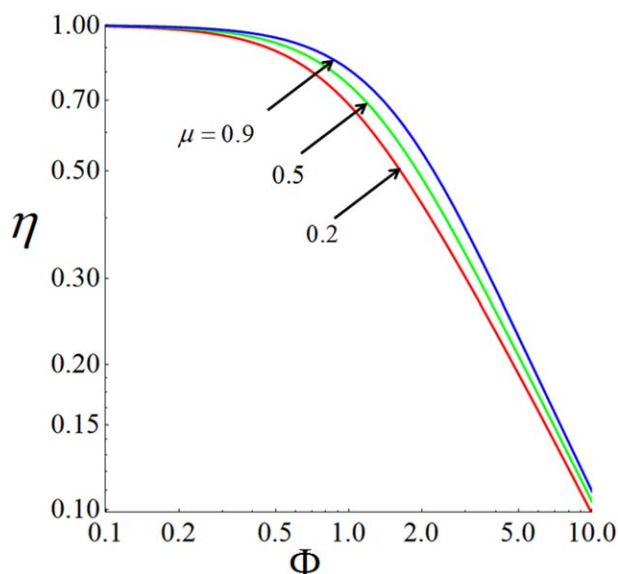


Figure 1. Effectiveness factor vs. the shape normalized Thiele modulus for a hollow cylinder with diffusion in the hole: $\delta = 0.1$ and $\mu = 0.2$ (red), 0.5 (green) and 0.9 (blue).

[Color figure can be viewed in the online issue, which is available at wileyonlinelibrary.com.]

A plot of η vs. Φ_* for the case of $\delta = 0$, $\lambda = 1$ for the same three values of μ (corresponding to the boundary condition used by WKW) is similar to that in Figure 1. These computations as well as the aforementioned analysis confirm the asymptotic behavior and the proper definition of the shape normalized Thiele modulus.

Geometric Limits

Before considering some geometric limits, we invoke a couple of identities involving infinite sums. By solving the effectiveness factor problem for infinite slab geometry directly and by using the Fourier transform method, it is easily shown that

$$\frac{\tanh \phi}{\phi} = 1 - \frac{8\phi^2}{\pi^2} \sum_{n=1}^{\infty} \frac{1}{(2n-1)^2 \left[\phi^2 + \frac{(2n-1)^2 \pi^2}{4} \right]} \quad (32)$$

Similarly, by solving the same problem in an infinite cylinder, it can be shown that

$$\frac{2I_1(\phi)}{\phi I_0(\phi)} = 1 - 4 \sum_{m=1}^{\infty} \frac{\phi^2}{j_m^2 [\phi^2 + j_m^2]} \quad (33)$$

where j_m is the m -th zero of the Bessel function $J_0(x)$.

The first geometric limit we consider is that of $\mu \rightarrow 0$, corresponding to that of solid cylinder. In this case, the effectiveness factor (for both $\delta = 0$ and $\delta > 0$) simplifies to

$$\eta = 1 - \frac{8\phi^2}{\pi^2} \sum_{n=1}^{\infty} \frac{1}{(2n-1)^2 \psi_n^2} \left[1 - \frac{2I_1(\psi_n)}{\psi_n I_0(\psi_n)} \right]$$

and using the identity given by Eq. 33, it reduces to the expression given by Aris.³ The second geometric limit of

interest is that of an infinite hollow cylinder ($\lambda \rightarrow \infty$). This limit is improper in that the two boundary conditions at the interior surface lead to different results. For $\delta > 0$, it may be shown that the expression reduces to

$$\eta = \frac{2}{\phi(1-\mu^2)} \frac{I_1(\phi)K_1(\mu\phi) - I_1(\mu\phi)K_1(\phi)}{I_0(\phi)K_1(\mu\phi) + I_1(\mu\phi)K_0(\phi)}, \quad (34)$$

while for $\delta = 0$ (or using the Dirichlet boundary condition at the interior circle), we get

$$\eta = \frac{2}{\phi^2(1-\mu^2)} \frac{[\phi Q_0(\mu\phi, \phi) + \mu\phi Q_0(\phi, \mu\phi) - 2]}{P_0(\phi, \mu\phi)} \quad (35)$$

Thus, as can be expected, in the limit of $\lambda \rightarrow \infty$, the effectiveness factor depends on the boundary condition used at the interior surface.

The third geometric limit of interest is that of $\lambda \rightarrow 0$, corresponding to a thin circular disk. We note that in this case, it is more appropriate to use $\lambda\phi$ as the modulus (or half thickness of the disk in place of outer radius). It may be shown that for this case, η is independent of μ and is given by

$$\eta = \frac{\tanh \lambda\phi}{\lambda\phi} \quad (36)$$

The last limiting case of interest is that of $\mu \rightarrow 1$, corresponding to a thin cylindrical shell. It may be shown that for this case

$$\eta = \frac{\tanh(1-\mu)\phi}{(1-\mu)\phi} \quad (37)$$

In particular, as can be expected intuitively, these last two limiting cases correspond to an infinite slab geometry and for any finite ϕ , η approaches unity as $\lambda \rightarrow 0$ or $\mu \rightarrow 1$. Figure 2 shows a schematic of the particle shape as μ and $\frac{1}{1+\lambda}$ are varied on the boundary of the unit square.

Aris Numbers and Geometry Factor

WKW define the zeroth Aris number (An_0) as the number that becomes equal to $\frac{1}{\eta^2}$ in the limit $\eta \rightarrow 0$. Thus

$$An_0 = \frac{1}{\eta^2}, \quad \eta \rightarrow 0 \quad (38)$$

It is clear from this definition, for the case of first-order kinetics, the zeroth Aris number is the square of the shape normalized Thiele modulus, i.e. $An_0 = \frac{1}{\eta^2} = \Phi^2$. As is well-known, the zeroth Aris number brings together the effectiveness factor curves in the limit of $\eta \rightarrow 0$. WKW also define the first Aris number as

$$An_1 = 1 - \eta^2, \quad \eta \rightarrow 1 \quad (39)$$

The first Aris number brings together the effectiveness factor curves in the limit of $\eta \rightarrow 1$. From the definition, it follows that

$$\eta^2 = 1 - An_1 = 1 - \Gamma\Phi^2 + O(\Phi^4) \quad \text{or} \quad (40)$$

$$\eta = 1 - \frac{\Gamma}{2}\Phi^2 + O(\Phi^4); \quad \Gamma = \frac{An_1}{An_0} \quad (41)$$

where Γ is termed as the geometry factor since it depends on the geometry (and/or aspect ratios) of the catalyst particle. It

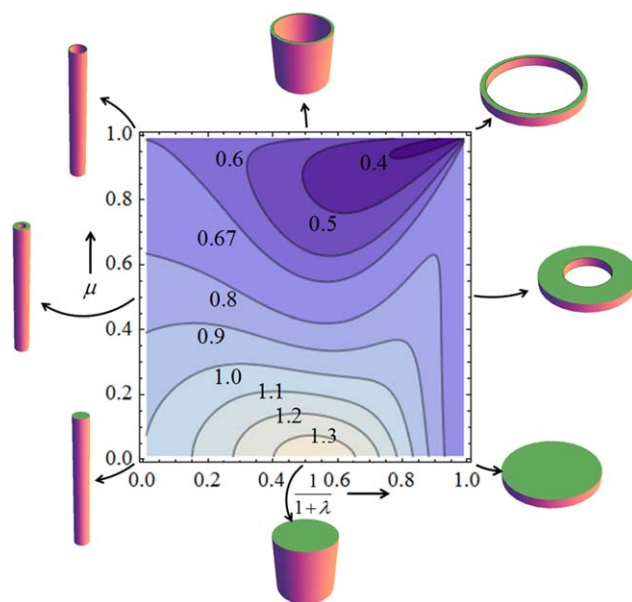


Figure 2. Contour plot of the geometry factor for the hollow cylinder for $\delta = 0.1$.

Also shown are the schematic shapes of the hollow cylinder for various aspect ratios on the boundary of the unit square. [Color figure can be viewed in the online issue, which is available at wileyonlinelibrary.com.]

follows from the aforementioned definitions that the shapes that lead to smaller values of Γ lead to higher effectiveness factors, and, hence, are favored. Also, as shown by Balakotaiah,⁵ the reciprocal of Γ determines the dimensionless mass-transfer coefficient (or the asymptotic Sherwood number) between the interior of the particle and its boundary. Thus, it is of interest to determine the geometry factor and its variation with the aspect ratios (λ, μ), and the diffusivity ratio (δ) for the case of hollow cylinder. This is examined in the following.

By expanding the expression for η given by Eq. 20 for small values of Φ , we obtain

$$\Gamma = \frac{64\lambda^2}{\pi^4(1-\mu^2)} \left[\frac{1}{\lambda} + \frac{2}{(1-\mu^2)} \right] \sum_{n=1}^{\infty} \frac{1-\mu^2+2\hat{\lambda}_n}{(2n-1)^4} \quad (42)$$

$$\hat{\lambda}_n = \frac{2 - [v_n Q_0(\mu v_n, v_n) + \mu v_n Q_0(v_n, \mu v_n)] + \delta v_n \frac{I_0(\mu v_n)}{I_1(\mu v_n)} P_1(\mu v_n, v_n)}{v_n^2 \left[P_0(v_n, \mu v_n) + \delta \frac{I_0(\mu v_n)}{I_1(\mu v_n)} Q_0(v_n, \mu v_n) \right]} \quad (43)$$

Once again, when the terms containing δ are excluded, this expression agrees with that derived by WKW. For the case of solid cylinder ($\mu=0$), it may be simplified to

$$\Gamma = \frac{2}{3}(1+2\lambda)^2 - \frac{256\lambda(1+2\lambda)^2}{\pi^5} \sum_{n=1}^{\infty} \frac{1}{(2n-1)^5} \frac{I_1(v_n)}{I_0(v_n)}. \quad (44)$$

We note that this value approaches the limit $\frac{2}{3}$ for $\lambda \rightarrow 0$ and 1 for $\lambda \rightarrow \infty$ corresponding to the infinite slab and cylinder limits. However, it is not a monotonic function of λ , attaining a maximum value of 1.36 at $\lambda \approx 0.85$. In other words, a finite cylindrical particle of aspect ratio 0.85 has the lowest effectiveness factor of any cylindrical particle!

Now, we consider a hollow particle of very large aspect ratio ($\lambda \rightarrow \infty$), or an annular region. In this case, Eq. 42 gives

$$\Gamma = \frac{1 - 3\mu^2 - \frac{4\mu^4 \log \mu}{(1-\mu^2)}}{(1-\mu^2)^2} (\delta > 0) \quad (45)$$

$$= \frac{2}{3} + \frac{1}{3}(1-\mu) + \frac{1}{10}(1-\mu)^2 + \dots \text{ for } \mu \rightarrow 1. \quad (46)$$

In this case, the geometry factor does not depend on δ and decreases monotonically from unity for $\mu \rightarrow 0$ to $\frac{2}{3}$ for $\mu \rightarrow 1$. While other limiting cases can be examined, we do not pursue them here. Instead, we present contour plots of Γ for some typical values of the diffusivity ratio δ . Figure 2 shows the variation of Γ with the aspect ratios λ and μ for the case of $\delta = 0.1$. As can be expected, for $\lambda \rightarrow 0$ or $\mu \rightarrow 1$ (the right and upper edges in Figure 2) Γ approaches the flat plate limit of $\frac{2}{3}$ while for $\mu \rightarrow 0$ (lower edge of Figure 2) it approaches the solid cylinder limit given by Eq. 44. For $\lambda \rightarrow \infty$ (left edge in Figure 2), it approaches the annulus limit given by Eq. 45. For any finite δ , the highest value (1.36) is the same as that attained for a solid cylinder, but the lowest value is different from that corresponding to the case considered by WKW. In the latter case, as shown by WKW, the lower bound for Γ is $\frac{2}{3}$. For $\delta = 0.1$, there is a large region bounded by a U-shaped contour that connects the upper two corners in Figure 2, in which Γ values are below $\frac{2}{3}$ (and as low as 0.4). It is found that this region exists for any $\delta < 1$, and the size of this region increases as δ is decreased. Thus, for a given ratio of the diffusivities δ there is an optimum shape (or aspect ratios λ and μ) that minimizes the geometry factor, and, hence, gives the highest effectiveness factor. While some of these shapes (e.g., thin cylindrical shells and rings) are not practical, others are in the practical range of interest (e.g., $\lambda = 1$ and $\mu = 0.5$ to 0.75), and have higher effectiveness than a thin disk or cylindrical shell/flat plate.

Summary

The main result of this work is an analytical expression for the effectiveness factor of a catalyst particle in the form of a hollow cylinder. We have also shown that the effective length-scale to be used in the definition of the generalized Thiele modulus is the ratio of reactive volume of the pellet to the total external area exposed to the reactant. This generalized definition also applies whether the nonreactive core extends to the external surface or is completely enclosed.

In this work, we considered only catalyst particles in the shape of hollow cylinders. One possible extension of this work could be generalization to particles with multiple holes or other shapes, including irregular and/or fractal shapes consisting of reacting as well as diffusion only regions. Based on this work, it appears that there is an optimum shape that maximizes the catalyst effectiveness and it depends on the diffusivity ratio.

Acknowledgments

This work was presented by late Professor Rutherford Aris at the AIChE meeting in Dallas in 1999 in a session honoring Prof. D. Ramkrishna of Purdue University. The authors dedicate this work to Professor D. Ramkrishna, who has shown the value of linear operator theory in solving Chemical Engineering problems. The work of V. Balakotaiah was supported by a grant from the Robert A. Welch Foundation (grant#E-1152).

Notation

Roman letters

a = inner radius of cylinder
 b = outer radius of cylinder
 C = reactant concentration
 D_e = effective diffusivity in the catalyst
 D_m = molecular diffusivity of reactant in the fluid phase
 I_0 = modified Bessel function of order zero
 I_1 = modified Bessel function of order one
 K_0 = Bessel function of order zero
 K_1 = Bessel function of order one
 k_0 = rate constant (first-order) based on unit catalyst volume
 L = half-length of particle
 R_Ω = effective average diffusion length
 U = dimensionless reactant conversion in the hole
 V = dimensionless reactant conversion in the annulus
 z = dimensionless axial position

Greek letters

Γ = geometry factor
 Φ = normalized Thiele modulus
 δ = ratio D_e/D_m
 ρ = dimensionless radial position
 λ = ratio of height to diameter
 μ = ratio of inner to outer radius
 η = effectiveness factor

Literature Cited

1. Wijngaarden RJ, Kronberg A, Westerterp KR. *Industrial Catalysis: Optimizing Catalysts and Processes.*, Weinheim, Germany: Wiley-VCH Verlag; 1998.
2. Gunn DJ. Diffusion and chemical reaction in catalysis and adsorption, *Chem Eng Sci.* 1967;22:1439–1455.
3. Aris R. *The Mathematical Theory of Diffusion and Reaction in Permeable Catalysts.* Oxford University Press; 1975.
4. Aris R, Balakotaiah V. Asymptotic Effectiveness of a Catalyst Particle in the form of a Hollow Cylinder. paper #238b, presented at AIChE Annual Meeting; Dallas, TX; 1999.
5. Balakotaiah V. On the relationship between Aris and Sherwood numbers and friction and effectiveness factors, *Chem Eng Sci.* 2008;63:5802–5812.

Manuscript received May 28, 2013, and revision received Aug. 10, 2013.

